ChemComm

# Visible-light-driven dry reforming of methane using semiconductor-supported catalyst



| | |
|---|---|
| Journal: | *ChemComm* |
| Manuscript ID | CC-COM-01-2020-000729.R1 |
| Article Type: | Communication |
| | |

COMMUNICATION

# Visible-light-driven dry reforming of methane using semiconductor-supported catalyst

Received 00th January 20xx,
Accepted 00th January 20xx

DOI: 10.1039/x0xx00000x

Yohei Cho,[a] Shusaku Shoji,[a] Akira Yamaguchi,[a] Takuya Hoshina,[a] Takeshi Fujita,[b] Hideki Abe[c] and Masahiro Miyauchi *[a]

**Dry reforming of methane (DRM) is an attractive reaction that consumes two major greenhouse gases while producing the industrially important components of syngas. In this study, various semiconductors were examined as light-harvesting support materials to promote catalytic DRM reaction under mild conditions. Among the metal-loaded catalysts, rhodium-loaded tantalum oxynitride (Rh/TaON) drove the DRM reaction even under visible light irradiation (>400 nm), and its activity exceeded the thermal catalyst limit. According to our spectroscopic analysis and the surface temperature measurement, the bandgap excitation of TaON dominantly promotes the DRM reaction in addition to its photo-thermal effect.**

Global warming poses a significant threat to life on earth, thus it is crucial to mitigate its causes. Greenhouse gases (especially carbon dioxide ($CO_2$) and methane ($CH_4$)) are the main origin of global warming. On the other hand, syngas, a mixture of hydrogen ($H_2$) and carbon monoxide (CO), is important for the industrial production of liquid fuel and chemicals. Since it consumes greenhouse gases and produces syngas, dry reforming of methane (DRM: $CH_4 + CO_2 \rightarrow 2H_2 + 2CO$) has garnered much attention recently.

However, DRM has severe limitations, including high operating temperatures or low long-term catalyst stability. Owing to its highly positive enthalpy value ($\Delta H_{298}$ = +247 kJ/mol), the reaction requires high temperatures even using a catalyst. Therefore, most DRM processes are carried out at temperatures higher than 700 °C.[1] However, higher temperatures usually leads to the aggregation of catalyst nanoparticles. In addition, conventional metal catalysts, such as nickel, are easily deactivated by carbon deposition so-called coking. To lower the operating temperature for DRM, previous studies have focused on optimizing catalyst composition and morphology, as well as improving catalyst support materials.[2] Despite these efforts, catalytic conversion and/or yield cannot exceed the theoretical thermodynamic limit. For example, the thermodynamic limit of $H_2$ yield for the present study is 36 % at 450 °C and ambient pressure using a $CH_4/CO_2/Ar$ = 1/1/98 input gas mixture.

Recent reports indicate that photon energy can assist DRM reactions at reduced operating temperatures. Takami et al. suggested that plasmonic metal nanoparticle catalysts can be used to accelerate DRM.[3] Similarly, Song et al. performed steam reforming of methane (SRM) using rhodium-modified titanium dioxide under light irradiation, and concluded that the SRM reaction was assisted by hot carriers generated in rhodium.[4] In contrast to plasmonic excitation of metals, several studies have reported a photocatalytic DRM reaction using interband transitions in metal oxide semiconductors. Wibowo et al. used pristine $SrTiO_3$ to demonstrate a clear photocatalytic effect,[5] reaching 3.8% methane conversion under 700 °C. Very recently, Shoji et al. reported that rhodium-loaded strontium titanate ($Rh/SrTiO_3$) exhibited 50% yield and conversion of DRM reaction under UV light irradiation below 150 °C; this greatly exceeds the theoretical thermodynamic limit.[6] Using electron spin resonance (ESR), they concluded that $SrTiO_3$ bandgap excitation played more dominant role than photothermal effects to drive the DRM reaction.[6] Although the DRM reaction was catalysed by $Rh/SrTiO_3$ at low temperatures, it still required UV irradiation.

In this study, we aim to develop a visible-light-sensitive photocatalyst to drive the DRM reaction with high conversion and/or yield, using metal catalysts supported on an appropriate semiconductor. According to our previous studies,[5, 6] the energy level of the conduction band (CB) of a metal oxide semiconductor is an important determinant in using photon irradiation to drive the DRM reaction. Firstly, we strategically chose various appropriate semiconductors to meet the requirements of a narrow bandgap and a high conduction band.

The semiconductors chosen for this study have demonstrated high efficiency in other photocatalytic systems, including $CO_2$ reduction, water splitting, and pollutant degradation. The list of candidates is shown in Table 1. P-type metal oxides like $ZnFe_2O_4$, $CaFe_2O_4$, and $Cu_2O$ are prospective candidates because of their narrow bandgaps and high conduction bands.

[a] *Department of Materials Science and Engineering, Tokyo Institute of Technology, 2-12-1 Ookayama, Meguro-ku, Tokyo 152-8552, Japan*
[b] *School of Environmental Science and Engineering, Kochi University of Technology, 185 Miyanokuchi, Tosayamada, Kami, Kochi 7 782-8502, Japan*
[c] *National Institute for Materials Science, 1-1 Namiki, Tsukuba, Ibaraki 305-0044, Japan*
† Electronic Supplementary Information (ESI) available. See DOI: 10.1039/x0xx00000x

**Table1. $H_2$ yield (%) over visible-light-sensitive catalysts with and without visible light irradiation at 450°C**

| light | CdS [7] | $Bi_2S_3$ [8] | TaON [9] | $Ta_3N_5$ [9] | Rh doped $SrTiO_3$ [10] | g-$C_3N_4$ [11] | $Bi_2WO_6$ [12] | $MgFe_2O_4$ [13] | $ZnFe_2O_4$ [13] | $CaFe_2O_4$ [13] |
|---|---|---|---|---|---|---|---|---|---|---|
| OFF | N.D. | N.D. | N.D. | N.D. | N.D. | N.D. | 1. 6 | 0.1 | N.D. | N.D. |
| ON | 1.2 | 0.21 | N.D. | N.D. | N.D. | 0.2 | N.D. | N.D. | N.D. | N.D. |
| light | $Cu_2O$ | Rh/ $Bi_2WO_6$ | Ru/ $ZnFe_2O_4$ | Ru/ $CaFe_2O_4$ | Rh/ $Cu_2O$ | Rh/ g-$C_3N_4$ | Rh/ TaON | Rh/ $Ta_3N_5$ | Thermal catalyst limit | |
| OFF | N.D. | N.D. | N.D. | N.D. | N.D. | N.D. | 15.6 | 22.8 | 36.3 | |
| ON | 0.6 | N.D. | 2.2 | 2.4 | N.D. | 0.1 | 50.3 | 33.6 | - | |

For example, the bandgap of $CaFe_2O_4$ is reported to be 1.9 eV, and its CB is
located at -0.6V (vs. NHE), thus it can reduce $CO_2$ under visible light irradiation, owing to its high conduction band.[14] Also, g-$C_3N_4$ has a high conduction band position (-1.23 V vs NHE) and is used as a visible-light-activated photocatalyst for water splitting. In addition, metal sulfides and nitrides such as CdS,[7] $Bi_2S_3$,[8] and $Ta_3N_5$[9] were chosen, since their valence bands are shallower than those of metal oxides and they are responsive to visible light. Furthermore, we chose the metal-ion-doped metal oxide, Rh-doped $SrTiO_3$,[10] since it is a well-known state-of-art visible-light-activated photocatalyst for overall water splitting. We deposited rhodium (Rh) or ruthenium (Ru) nanoparticle catalysts onto these light-harvesting catalyst supports using a conventional impregnation method. Our procedure for evaluating catalysts is described in the Supporting Information.

Table 1 shows the yield of $H_2$ for various catalysts under both visible light irradiation and dark conditions at 450 °C using a flow reactor (described in Supporting Information, Scheme S1 and S2). Visible light spectra are shown in the Supporting Information (Fig. S1). The theoretical highest yield under the present experimental conditions is 36.3 %, as calculated by thermodynamic simulation software.[15] Several important results are demonstrated in Table 1. Firstly, the DRM reaction does not proceed using pristine semiconductors. Secondly, in case of Rh or Ru loaded catalyst, catalytic activity was significantly influenced by the semiconductor support, even under dark conditions. Among the supports, tantalum-based oxynitride (TaON) and nitride ($Ta_3N_5$) deposited with Rh nanoparticles exhibited efficient DRM activities under both dark and visible-light irradiation conditions. Visible light irradiation of Rh/TaON largely enhanced its activity as compared to that under dark condition, and its $H_2$ yield under visible light (50.3 %) significantly exceeded the theoretical thermal catalyst limit. We also observed that Rh-loaded tantalum-based oxynitride and nitride exhibited superior DRM activities, even under dark conditions. According to previous studies, interaction between the metal and semiconductor support is an important factor. Nakagawa et al. reported the effect of support materials on a iridium catalyst for methane conversion,[16] and determined the order of performance ranged in the order $TiO_2 \geq ZrO_2 \geq Y_2O_3 > La_2O_3 > MgO \geq Al_2O_3 > SiO_2$. On the other hand, Ruckenstein et al. reported the effect of the catalyst support on DRM with Rh catalysts,[17] and measured activities in the order of $SiO_2 \approx MgO \approx \gamma\text{-}Al_2O_3 > Y_2O_3 > Ta_2O_5 \approx La_2O_3 > TiO_2 > ZrO_2 > Nb_2O_5 > CeO_2$. Catalytic performance was strongly influenced by the ability of the support material to be reduced. Since $SiO_2$ was the best support for the DRM reaction using the Rh catalyst, we also prepared a $Rh/SiO_2$ catalyst as a control. It generated a yield of 11.1% $H_2$ at 450 °C (Supporting Information, Fig. S2). The yields of our Rh/TaON and $Rh/Ta_3N_5$ catalysts were comparable to that of conventional $Rh/SiO_2$, even under dark conditions. Thus, these catalysts were chosen for further study; their structural and optical properties and their photocatalytic reaction mechanism was investigated in detail.

Here, we briefly describe the preparation and characterization of TaON and $Ta_3N_5$. TaON powder was prepared by heat treating $Ta_2O_5$ powder under a gaseous ammonia flow; $Ta_3N_5$ was purchased from Kojundo Chemical Lab. Co., Ltd. Next, rhodium particles were deposited onto TaON and $Ta_3N_5$. The deposition method was optimized for high DRM activity, then the hydrothermal method was better than the impregnation or photo-deposition methods (see our Supporting Information, Fig. S3), because of the high dispersion of Rh nanoparticles (Fig. S4 and S5). We also optimized the amount of Rh for visible light DRM activity, and 5 wt% (precursor amount) showed the best performance (Fig. S6). Its actual Rh loaded amount on TaON was measured using ICP analysis, which turned out to be 0.68 wt% (See Supporting Information for more detailed measurement condition). Fig. 1(a) and Fig. S7 show UV-Vis absorption spectra. Steep absorption edges are observed in the spectra of these materials; this signal results from the bandgap excitation of semiconductors. Tauc plots (shown in Supporting Information Fig. S8 and S9) were constructed based on these absorption spectra, and the bandgaps of TaON and $Ta_3N_5$ are estimated to be 2.7 and 2.1 eV, respectively. Domen et al. previously reported that the nitrogen 2p orbital is located above the oxygen 2p orbital in tantalum-based oxynitride, and that nitrogen-doping induced an upshift in the valence band and

 

narrowing of the bandgap, while maintaining its high conduction band position.[9] Our optical results are consistent with this previous report; TaON and $Ta_3N_5$ absorb visible light. Transmission electron microscopy (TEM) indicates that rhodium nanoparticles were well dispersed onto the TaON surface, as shown in Fig. 1(c) and (d) The presence of rhodium was also confirmed by energy dispersive X-ray spectroscopy (EDS) analysis (Supporting Information, Fig. S10). In addition, we performed X-ray diffraction (XRD) and hard X-ray photoelectron spectroscopy (HAXPES) with $Ta_2O_5$, TaON, and $Ta_3N_5$ (see the Supporting Information, Fig. S11–S14). The XPS signals for Ta 4d shifted to higher binding energy following the order $Ta_2O_5$, TaON, and $Ta_3N_5$. HAXPES spectra for N 2p and O 2p core-level orbitals confirm that the amount of nitrogen species increased by nitridization.

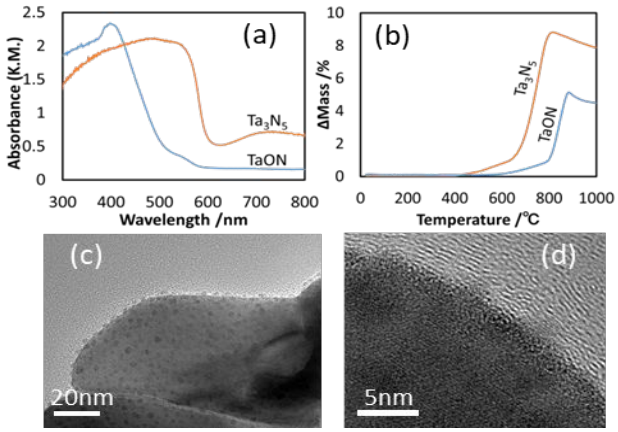


Fig. 1(a) UV-vis spectra of pristine TaON, and $Ta_3N_5$. (b) Results of TG-DTA analysis on TaON and $Ta_3N_5$ recorded in air atmosphere. (c)TEM image and (d) HR-TEM of Rh/TaON.

Fig. 1(b) shows the thermal stability of TaON and $Ta_3N_5$ as analyzed by thermogravimeter-differential thermal analyzer (TG-DTA) under ambient air condition. Weight gain during heat treatment was observed in these samples, owing to the replacement of nitrogen with oxygen ions. $Ta_3N_5$ had lower thermal stability than TaON, which was stable below 600 °C, and the nitrogen ions in $Ta_3N_5$ were significantly replaced by oxygen, even at approximately 400 °C in air. Indeed, the catalytic performance of Rh/TaON at high temperature under dark condition was higher than that that of Rh/$Ta_3N_5$ (Fig. S15 and S16 in Supporting Information). Also, from Table 1, Rh/TaON has higher photocatalytic activity under visible light irradiation than Rh/$Ta_3N_5$, owing to the stronger oxidation power of TaON with its deeper valence band,[9] and highly dispersed Rh nanoparticles onto TaON rather than those onto $Ta_3N_5$ (Fig. S17 in Supporting Information). Thus, we chose TaON as a catalyst support for further study and examined its photocatalysis mechanism in detail.

Fig. 2(a) shows the temperature-dependence of $H_2$ yields for DRM using gas flow conditions with the Rh/TaON catalyst. The dashed line represents the maximum theoretical yield under consideration on equilibrium for the present condition. Under dark conditions, $H_2$ yield was less than the theoretical limit. In contrast, $H_2$ production under visible light irradiation exceeded the thermal catalyst limit. These results clearly indicate that visible light stimulates the DRM reaction, even at low temperature. The photocatalytic activity depended on the light intensity (Fig. S18, Supporting Information). Figure 2(b) shows the long-term durability test under light irradiation. The high yield of Rh/TaON was maintained for 12 h, and the turnover number for the photocatalyst was estimated to be 2120, indicating the high stability of our photocatalyst. It is noted that the rate of $H_2$ and CO production was consistent and was twice of the consumption rate of $CH_4$ and $CO_2$ (Fig. 2(c), Fig. S19), indicating its stoichiometric DRM conversion without coking. We also observed the TEM images after the 8 h reaction at 450 °C (Fig. S20 in Supporting Information), and there was neither significant aggregation of Rh nanoparticles nor coking.

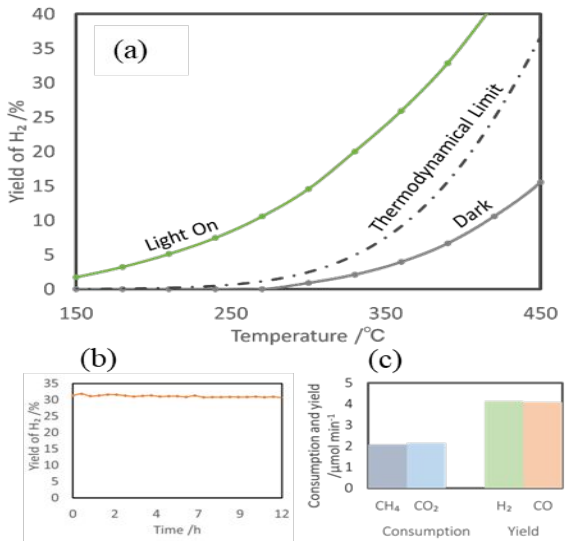


Fig. 2(a) DRM activities of Rh/TaON under dark condition (grey) and under visible light irradiation (green). The black line represents the thermodynamic limit for $H_2$ yield under the present experimental conditions. (b) Stability test of Rh/TaON under visible light irradiation at 400 °C. (c) Consumption and production rates for each gas.

To verify the catalysis mechanism, we measured the surface temperature of the catalysts under visible light irradiation using a radiation thermometer (Fig. S21 in Supporting Information), then the surface temperature was 316 °C, when the bulk (reactor) temperature was set at 210 °C. Thus, we compared the DRM activity under light irradiation with that under the dark condition at the same surface temperature (316 °C), and the results are shown in Fig. 3(a). It should be noted that the dark condition would have more advantage, since the heat treatment was applied to the whole bulk catalyst in a reactor. However, the yield of $H_2$ under light irradiation condition was 3.3 times as high as the later dark condition as shown in Fig. 3(a). Another evidence to support photocatalysis mechanism is that the loading amount of Rh was optimum at 5% under light irradiation, whereas the activity increased monotonically under dark condition (Fig. S6),

revealing the different trend between light irradiation and dark condition. Furthermore, the activities of Rh loaded photocatalysts other than Rh/TaON were almost negligible under light irradiation (Table 1), indicating that the photo-absorption in Rh did not so contribute to the DRM activities. These results indicate that the high activity under light irradiation is not simply explained by a thermal process.

We also measured the surface temperature along with the different wavelength to investigate the photothermal effect triggered by the irradiated light (spectra shown in Fig. S22 in Supporting Information). And as a result, the surface temperature gradually increased as the shorter cutoff filter was used (Fig. S23). As for comparison, the surface temperature of Rh loaded ultra-widegap $Al_2O_3$, which was not excited under the present light irradiation, was measured. Then, Rh/TaON exhibited slightly higher surface temperature than Rh/$Al_2O_3$ in the wavelength attributed to the bandgap excitation as well as the recombination in TaON. These results imply that the thermal effects under light irradiation, including plasmon absorption in Rh and recombination of electron-hole pairs in TaON partly contribute to the efficient DRM reaction under visible light irradiation. Figure 3 (b) shows the action spectrum for $H_2$ yield under the specific wavelength using cutoff filters (spectra shown in Fig. S22 in Supporting Information). Indeed, the results clearly show that the DRM activities of Rh/TaON are boosted by visible light irradiation. The enhanced DRM activity of Rh/TaON under visible light irradiation is dominantly attributed to its photocatalytic electron-hole pairs in addition to the photothermal effect, since Shoji et al. recently reported a similar trend for the Rh/$SrTiO_3$ photocatalyst under UV irradiation.[6] According to their in-situ electron spin resonance (ESR) spectroscopy results, excited electrons in the conduction band reduced $CO_2$, while holes generated in the valence band oxidized $CH_4$. They also investigated the DRM redox reaction mediator via isotope trace analysis using $^{18}O$ ion-doped $SrTiO_3$. Lattice oxygen ions near the metal oxide support surface acted as the redox mediator for the overall DRM reaction on the Rh catalyst. In our TaON system, oxygen defects would play an important role in promoting an efficient, visible-light-driven DRM reaction.

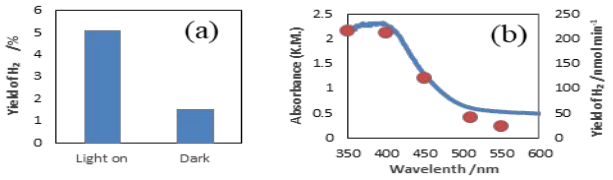


Fig. 3 (a) Comparison of activity under light irradiation condition (Surface temperature=316 °C, operating temperature=210 °C) vs dark condition (Surface temperature=operating temperature=316°C). (b) Action spectrum of Rh/TaON and UV-vis absorption spectra for Rh/TaON.

In conclusion, Rh/TaON exhibited efficient DRM under visible light irradiation compared to various visible-light-sensitive photocatalysts. DRM activity of Rh/TaON irradiated using a Xe lamp passed through a UV cut-off filter exceeded the theoretical thermodynamic catalyst performance limit. The photocatalyst was stable, with a turnover number of 2120, and drove stoichiometric syngas generation. While the photothermal process contributed to the high DRM activity under visible light irradiation, bandgap excitation in TaON plays a significant role in the present system.

This work was financially supported by Japan Science and Technology Agency (JST) CREST (No. JPMJCR15P1) and Japan Society for the Promotion of Science (JSPS) Kakenhi (No. 18H02055). We appreciate Mr. Genseki and Ms. Otsuka for their kind help to perform TEM and ICP analysis shown in this paper. The HAXPES analysis was carried out with the cooperation of Dr. Ueda at the NIMS beamline (BL15XU) in the SPring-8 synchrotron radiation facility, Japan.

## Conflicts of interest

There are no conflicts to declare.

## Notes and references

1. N. Laosiripojana and S. Assabumrungrat, *Applied Catalysis B: Environmental*, 2005, **60**, 107-116.
2. Y. Wang, L. Yao, S. Wang, D. Mao and C. Hu, *Fuel Processing Technology*, 2018, **169**, 199-206.
3. D. Takami, Y. Ito, S. Kawaharasaki, A. Yamamoto and H. Yoshida, *Sustainable Energy & Fuels*, 2019, DOI: 10.1039/C9SE00206E.
4. H. Song, X. Meng, Z.-j. Wang, Z. Wang, H. Chen, Y. Weng, F. Ichihara, M. Oshikiri, T. Kako and J. Ye, *ACS Catalysis*, 2018, **8**, 7556-7565.
5. S. Wibowo, A. Yamaguchi, S. Shoji, T. Fujita, H. Abe and M. Miyauchi, *Chemistry Letters*, 2018, **47**, 935-937.
6. S. Shoji, X. Peng, A. Yamaguchi, R. Watanabe, C. Fukuhara, Y. Cho, T. Yamamoto, S. Matsumura, M.-W. Yu, S. Ishii, T. Fujita, H. Abe and M. Miyauchi, *Nature Catalysis*, 2020, **3**, 148-153.
7. Y. Li, F. Huang, Q. Zhang and Z. Gu, *Journal of Materials Science*, 2000, **35**, 5933-5937.
8. H. Kim, J.-e. Park, K. Kim, M.-K. Han, S.-J. Kim and W. Lee, *Chinese Journal of Chemistry*, 2013, **31**, 752-756.
9. W.-J. Chun, A. Ishikawa, H. Fujisawa, T. Takata, J. N. Kondo, M. Hara, M. Kawai, Y. Matsumoto and K. Domen, *The Journal of Physical Chemistry B*, 2003, **107**, 1798-1803.
10. R. Konta, T. Ishii, H. Kato and A. Kudo, *The Journal of Physical Chemistry B*, 2004, **108**, 8992-8995.
11. S. Cao, J. Low, J. Yu and M. Jaroniec, *Advanced Materials*, 2015, **27**, 2150-2176.
12. Y. Zhou, Z. Tian, Z. Zhao, Q. Liu, J. Kou, X. Chen, J. Gao, S. Yan and Z. Zou, *ACS Applied Materials & Interfaces*, 2011, **3**, 3594-3601.
13. E. Casbeer, V. K. Sharma and X.-Z. Li, *Separation and Purification Technology*, 2012, **87**, 1-14.
14. Z. Liu, Z.-G. Zhao and M. Miyauchi, *The Journal of Physical Chemistry C*, 2009, **113**, 17132-17137.
15. S. Gordon and B. J. McBride, *NASA Reference Publication 1311*, 1994.
16. K. Nakagawa, K. Anzai and N. Matsui, *Catalysis Letters*, Catalysis Letters, **51**, 163–167.
17. H. Y. Wang and E. Ruckenstein, *Applied Catalysis A: General*, 2000, **204**, 143-152.

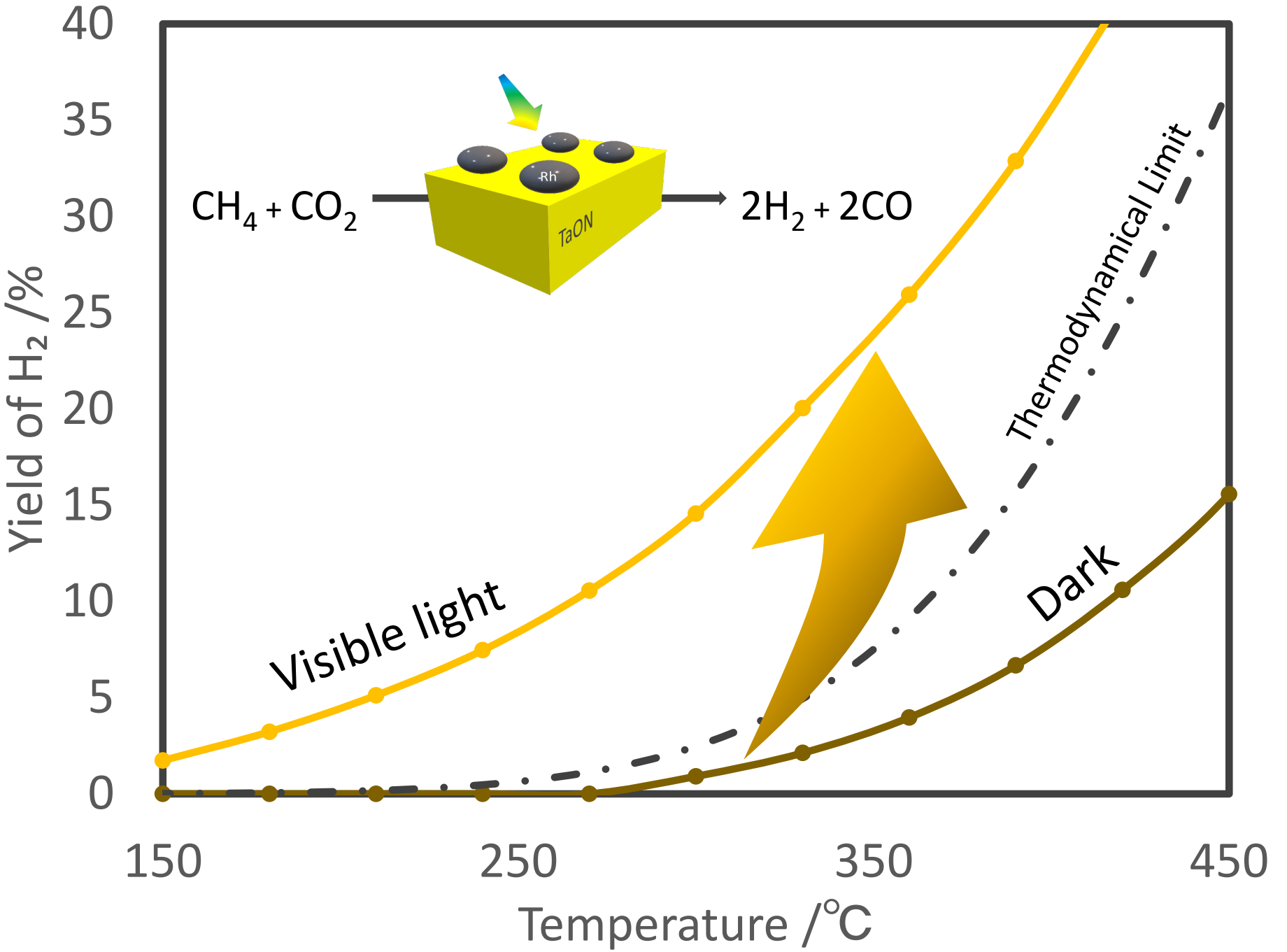
40
35
30
25
20
15
10
5
0
Yield of H2 /%
150
250
350
450
Temperature /°C
CH4 + CO2
2H2 + 2CO
Rh
TaON
Visible light
Dark
Thermodynamical Limit